

Magnetism and charge ordering in $\text{Fe}_3\text{O}_2\text{BO}_3$ studied by ^{57}Fe Mössbauer spectroscopy

J. Larrea J.,¹ D. R. Sánchez,¹ F. J. Litterst,^{1,*} E. M. Baggio-Saitovitch,¹ J. C. Fernandes,²
R. B. Guimarães,² and M. A. Continentino²

¹Centro Brasileiro de Pesquisas Físicas, Rua Dr. Xavier Sigaud 150, Rio de Janeiro, 22290-180, RJ, Brazil

²Instituto de Física, Universidade Federal Fluminense, Campus da Praia Vermelha, Niterói, 24210-340, RJ, Brazil

(Received 31 March 2004; revised manuscript received 9 August 2004; published 24 November 2004)

The homometallic Fe ludwigite $\text{Fe}_3\text{O}_2\text{BO}_3$, is an oxyborate with a chain structure of oxygen octahedra occupied by Fe^{2+} and Fe^{3+} with four different crystallographic sites. We report ^{57}Fe Mössbauer spectroscopic studies on the magnetic spin arrangements and on the charge ordering in $\text{Fe}_3\text{O}_2\text{BO}_3$, between 4 and 450 K. From the temperature dependence of the isomer shifts and quadrupole interactions, together with the information from previous x-ray and transport data, we are able to discuss the structural arrangement of Fe^{2+} and Fe^{3+} and the dynamics of the electronic configurations. Below $T_{N1} = 112$ K the Mössbauer spectra show the onset of antiferromagnetic order only for a fraction of the Fe ions, the complementary fraction remaining paramagnetic down to 74 K. Below 74 K all the sample becomes magnetically ordered, and an increase and a canting of the magnetic hyperfine field for each Fe ion is observed. This canting is related to the presence of weak ferromagnetism, as proposed from magnetization measurements. Below ~ 50 K antiferromagnetic order is found. From Mössbauer spectra taken under applied external magnetic fields, there is strong evidence for magnetic short-range order above T_{N1} involving ferromagnetic clusters. The observed magnetic transitions appear to be clearly related to charge ordering.

DOI: 10.1103/PhysRevB.70.174452

PACS number(s): 75.30.Kz, 76.80.+y, 73.20.Jc

I. INTRODUCTION

Research in metal oxides has been intensified considerably after the discovery of high critical temperature superconductivity and giant magnetoresistance.¹ Particularly, charge ordering, electron delocalization, and unusual magnetic order occur in Fe oxides, with valence fluctuations making these materials even more interesting from the physical point of view. Oxyborates exhibit properties determined by a combination of strong correlations and low-dimensional effects.² They form a family of compounds having several chemical compositions with at least ten known different crystalline structures. Those having the general chemical formula $M^{2+}M^{3+}\text{OBO}_3$ crystallize as warwickites, while the ludwigites have a general formula $M^{2+}M^{3+}\text{O}_2\text{BO}_3$.

$\text{Fe}_3\text{O}_2\text{BO}_3$, which is known as *homometallic Fe ludwigite*, has a crystal structure basically formed by an assembly of subunits in the form of *zigzag walls* built from four kinds of edge-sharing nonequivalent oxygen octahedra (see Fig. 1).²⁻⁵ The sites in their centers, labeled 1–4 in the following, are occupied by divalent (1 and 4) or trivalent (2 and 3) Fe ions. The sequence of 3-2-3 sites forms a so-called *triad* that can be described as three Fe^{3+} sharing an extra electron. Evidence for this distribution comes from x-ray diffraction and from a first Mössbauer study of this compound reported in 1983 by Swinnea and Steinfink.⁵ The relative weights of the different sites are 1/6 for Fe(1), 1/6 for Fe(2), 1/3 for Fe(3), and 1/3 for Fe(4).

The triads are linked closely to one another forming three-leg ladders within the “walls” along the c axis. These ladders are responsible for the transport properties of the system, which can be described by an activated behavior with a strong change of the activation energy around 220 K, indicating a crossover temperature.⁶ At $T_{co} \approx 300$ K a clear tran-

sition appears in the electronic state of the three Fe ions as seen by Mössbauer spectroscopy,³ which could be of structural origin. Careful x-ray diffraction done on a single crystal could indeed relate this to a structural transition⁴ characterized by an alternate dimerization of the rungs in the ladder with a consequent doubling of the cell parameter in the c direction.

Magnetization measurements⁶ and our more recent Mössbauer data⁷ define three characteristic temperatures for the magnetic behavior at 112, 74, and 50 K. From Mössbauer spectra, an onset of magnetic hyperfine splitting is found at $T_{N1} = 112$ K (phase AF1)—a transition which, however, is hardly visible in susceptibility. A transition to a weak ferromagnetic phase (WF) at $T_{N2} \sim 70$ K is clearly traced from

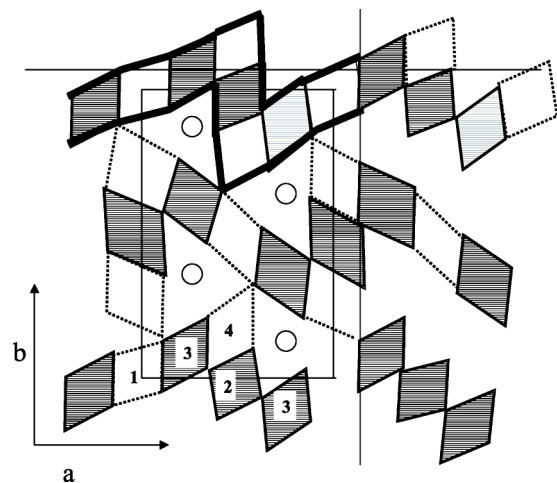


FIG. 1. Projection of the ludwigite structure to the ab plane. The four different crystallographic sites occupied by Fe ions are indicated. The triad is formed by sites 3-2-3.

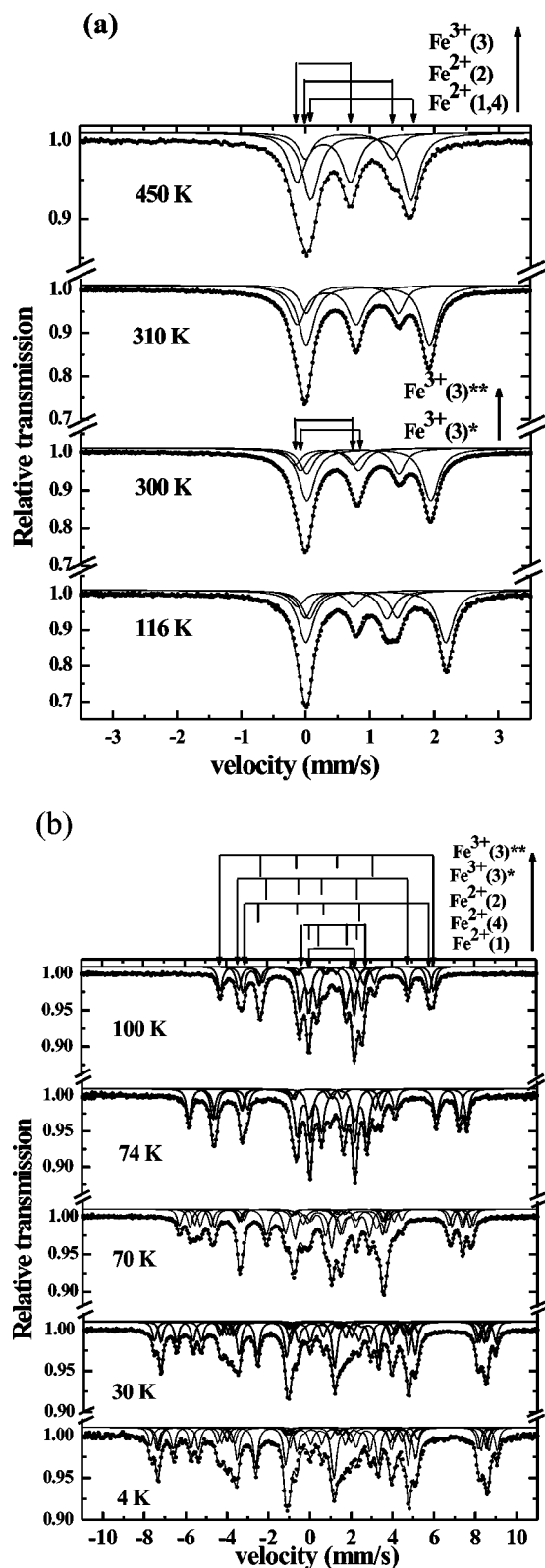


FIG. 2. Temperature dependence of the Mössbauer spectra of the ludwigite $\text{Fe}_3\text{O}_2\text{BO}_3$ (a) for $T > 116$ K and (b) for $T < 116$ K.

Mössbauer spectroscopy and also from a typical sharp signal in the ac susceptibility.^{6,8} The maximum of χ_{ac} has a negligible frequency dependencies, implying that there is indeed a magnetic phase transition and not a progressive freezing of

the magnetic moments. At T_{N2} the magnetization (in 1000 Oe applied field) rises sharply, reaches a maximum, and then slowly drops with decreasing temperatures reaching again the values found above the transition. Below T_{N2} the magnetization is clearly history dependent. In addition, there appears a spontaneous magnetization and a hysteresis loop below about 70 K, which vanishes again below approximately 40–50 K, indicating a reentrant antiferromagnetic state (AF2). This is in some contradiction to earlier neutron diffraction measurements on $\text{Fe}_3\text{O}_2\text{BO}_3$,⁹ which have shown that at 5 K the iron ions in sites 1 and 4 are ordered ferromagnetically, whereas the iron ions in the triads are antiferromagnetically coupled.

In this paper, we focus on the electronic and magnetic properties studied by Mössbauer spectroscopy. The temperature dependences of the isomer shift and of the quadrupole splitting can be very sensitive to transitions between ordered and disordered charge states. A transition of this kind has been proposed to occur in the Fe ludwigite based on transport measurements.⁴ Therefore, we have studied the temperature dependencies of the Mössbauer parameters searching for further evidence of charge ordering and their correlation with the magnetic transitions in the Fe ludwigite. Moreover, we extended the ^{57}Fe Mössbauer spectroscopic investigations to lower temperatures and also under external magnetic field in order to study the magnetic properties of $\text{Fe}_3\text{O}_2\text{BO}_3$ more thoroughly. Some preliminary results of our investigation have been reported in Ref. 7 and were meanwhile corroborated by another Mössbauer study by Douvalis *et al.*¹⁰ Mainly below about 80 K there are, however, clear qualitative differences between their and our results, leading to a different picture of the low temperature electronic state.

II. EXPERIMENTAL PROCEDURE

The preparation of the $\text{Fe}_3\text{O}_2\text{BO}_3$ samples is described elsewhere.⁶ Their characterization by x-ray diffraction at 300 K, indicates a single-phase material with the ludwigite structure.

^{57}Fe Mössbauer spectra were taken with the $\text{Fe}_3\text{O}_2\text{BO}_3$ sample kept in a variable temperature helium cryostat, in the range from 4.2 to 310 K, and in a vacuum-sealed oven, in the range from 295 to 450 K. The ^{57}Co :Rh source was kept at room temperature, moving in sinusoidal mode outside of the cryostat or the oven. Due to the large number of resonance lines appearing in the low-temperature spectra, the number of channels to collect the data was extended to 2048 in order to achieve a better resolution. Some spectra have been recorded under application of an external field of 7 T oriented along the direction γ -ray observation.

III. RESULTS AND DISCUSSION

A series of Mössbauer spectra of $\text{Fe}_3\text{O}_2\text{BO}_3$ was obtained between 4 and 450 K. Some representative ones, for the paramagnetic (PM) (a) and magnetic phases (b), are shown in Fig. 2. In the temperature range $113 \text{ K} < T < 450 \text{ K}$ the spectra are typical for a paramagnetic regime. We decided to

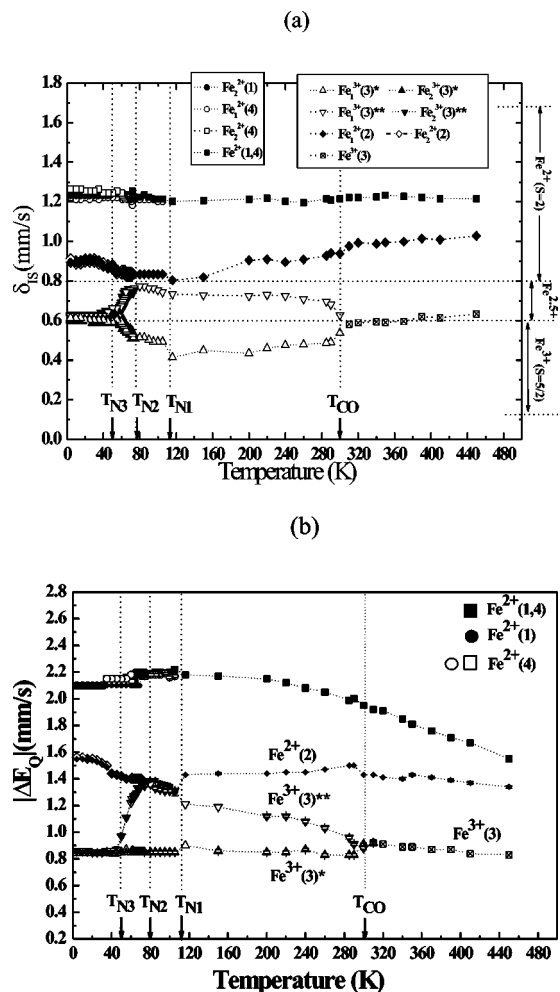


FIG. 3. Temperature variation of (a) isomer shift (δ_{IS}) and (b) quadrupole splitting (ΔE_Q) for the Fe ludwigite.

distinguish separate intervals of temperature with different fitting strategies, as described below.

A. The paramagnetic spectra

To analyze the Mössbauer spectra (MS) in the temperature range between 300 and 450 K, three doublets were considered. From the isomer shift (δ_{IS}) and quadrupole splitting (ΔE_Q) values (Fig. 3), two of the doublets can be assigned to high-spin Fe^{2+} , and the third to high-spin Fe^{3+} , all of them having octahedral oxygen coordination.¹¹ In this temperature range, the relative area of Fe^{2+} is $\sim 50\%$, in agreement with the charge balance per chemical formula for Fe^{2+} in sites 1 and 4.^{3,12} This, together with the behavior at low temperatures, leads us to attribute one of the Fe^{2+} doublets to sites 1 and 4. Because the δ_{IS} and ΔE_Q values are identical in the whole paramagnetic range, it is not possible to distinguish $\text{Fe}^{2+}(1)$ and $\text{Fe}^{2+}(4)$. Therefore, we will call this component $\text{Fe}^{2+}(1,4)$. Since it has a regular variation of δ_{IS} and ΔE_Q , we conclude that it is not related with charge ordering and delocalization effects [see Figs. 3(a) and 3(b)]. The remaining doublets are attributed to the Fe ions belonging to the triads. One has a δ_{IS} value typical of Fe^{3+} , while the other lies

between divalent and trivalent iron. They will be named $\text{Fe}^{3+}(3)$ and $\text{Fe}^{2+}(2)$, respectively. Above $T_{CO} \approx 300$ K the $\text{Fe}^{3+}(3)$ doublet has double intensity compared with $\text{Fe}^{2+}(2)$, thus, the extra electron in the triads may be considered to be located mainly in the columns of sites 2, the central sites of the triads. In the range $113 \text{ K} < T < 300 \text{ K}$, i.e., below the charge delocalization transition,³ it is necessary to introduce a fourth doublet to fit the MS. The three irons of the triad can now be distinguished since the two $\text{Fe}^{3+}(3)$ sites in a triad reveal different δ_{IS} and ΔE_Q values. The doublet having larger δ_{IS} and ΔE_Q values is named $\text{Fe}^{3+}(3)^{**}$ and the one with the smaller values, $\text{Fe}^{3+}(3)^*$. According to their isomer shift values, $\text{Fe}^{2+}(2)$ and $\text{Fe}^{2+}(3)^{**}$ are mixed valent, with valences close to a value of 2.5. The spectral weights for $\text{Fe}^{3+}(3)^*$ and $\text{Fe}^{3+}(3)^{**}$ are equal and add up to that of $\text{Fe}^{3+}(3)$ found at higher temperatures. Before continuing our discussion of the charge distribution in the Fe ludwigite structure, we will describe the magnetic spectra in order to establish the magnetic structure of $\text{Fe}_3\text{O}_2\text{BO}_3$ and combine it with the charge order transitions.

B. The magnetic spectra at zero external field

When cooling down the sample below $T_{N1} \approx 112$ K, a complex ^{57}Fe Mössbauer spectrum split by magnetic hyperfine interactions appears [Fig. 2(b)] indicating the onset of magnetic order. In order to fit the data in the temperature range $74 \text{ K} \leq T \leq 105 \text{ K}$, five sites were considered: four with combined electrical and magnetic interactions and a paramagnetic one. Taking into account the hyperfine parameters of the paramagnetic doublets above T_{N1} , the following attributions were made: the paramagnetic site corresponds to the Fe^{2+} at sites 1 [$\text{Fe}^{2+}(1)$], the other divalent Fe sites showing a magnetic hyperfine interaction belong to positions 4 [$\text{Fe}^{2+}(4)$]. The present results clearly show that the $\text{Fe}^{3+}(3)^*$ and the mixed valent ions $\text{Fe}^{2+}(2)$ and $\text{Fe}^{3+}(3)^{**}$ order magnetically at $T_{N1} \approx 112$ K.

For the analysis of the spectra with combined magnetic and quadrupole interactions, we used the eigenvalues and eigenvectors derived from the diagonalization of the full hyperfine Hamiltonian allowing for an angle θ between the magnetic hyperfine field B_{hf} and the main axis of the electric field gradient produced by the different octahedral oxygen coordination around the individual iron sites. In view of the large number of parameters, we tried to restrict them to a minimum, as already accomplished in Ref. 7. Douvalis *et al.*¹⁰ followed a similar method, but introduced additional fit parameters. Although these may be justified for describing the full Hamiltonian, they cannot, from first principles, all be determined from one spectrum. As shown in Ref. 13, at best five hyperfine parameters can be independently determined in the case of the nuclear spin 3/2 to 1/2 transition of ^{57}Fe . We will concentrate in the present context on the most essential results from our analysis. Details and a complete set of data will be made available elsewhere.

In Fig. 4 the magnetic hyperfine fields B_{hf} of the magnetically ordered Fe ions are plotted as function of temperature. Below 112 K the magnetic hyperfine fields for the $\text{Fe}^{3+}(3)^*$ ions and the two mixed valent ions $\text{Fe}^{2+}(2)$ and $\text{Fe}^{3+}(3)^{**}$

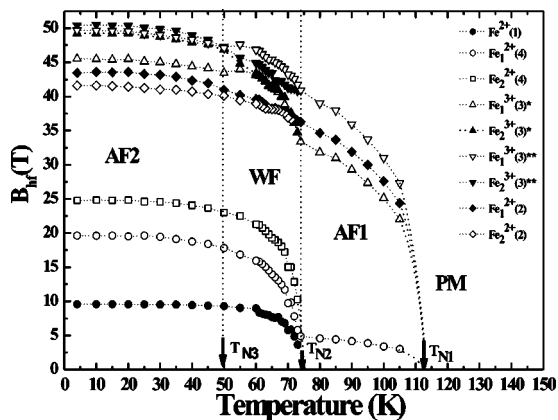


FIG. 4. Magnetic hyperfine fields as a function of temperature for the different magnetically ordered Fe ions. The dashed lines serve as guides for the eye.

follow the temperature dependence of regular sublattice magnetization curves, reaching values of 33, 36, and 41 T at 74 K, respectively.

Below 74 K a small but significant increase of B_{hf} at the $Fe^{2+}(2)$ and $Fe^{3+}(3)^{**}$ ions is observed and an even more pronounced one for the $Fe^{3+}(3)^*$ (Fig. 4). Below this temperature all magnetic sextets except for $Fe^{2+}(1)$ are split into two sextets with equal spectral weight and with the same δ_{IS} and ΔE_Q but different B_{hf} and angles θ . This can be interpreted with the formation of two fractions at two magnetically inequivalent sites for each of these iron sites. In Fig. 5, we show the temperature dependence of the angle θ for the different iron sites.

The other subsystem formed by Fe^{2+} in sites 1 and 4 behaves in a different way. For $112 K \geq T \geq 74 K$ only the Fe^{2+} ions in sites 4 are magnetically ordered and the hyper-

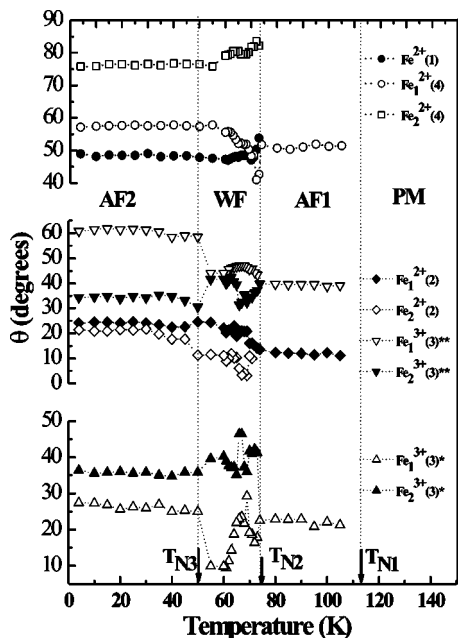


FIG. 5. Temperature dependence of the angles θ between B_{hf} and V_{zz} .

fine field values follow a regular magnetization curve, approaching a relatively low saturation value at $B_{hf}(74 K) = 5 T$. Below this temperature, analogous to the Fe ions in the triads 3-2-3, their corresponding magnetization curve splits in two (Fig. 4), implying that there are two fractions of Fe^{2+} ions in sites 4, each one with different magnetic hyperfine field and of equal spectral weight. Below 74 K, for one fraction of $Fe^{2+}(4)$ there is a more pronounced increase of B_{hf} than for the other. In addition, the angles θ reveal different temperature dependencies (Fig. 5). The Fe^{2+} ions in sites 1 are the only ones to remain paramagnetic down to 74 K, but below this temperature they also order magnetically. Lowering the temperature, their B_{hf} increases, following a regular magnetization curve, and reaches saturation at $\sim 40 K$ (Fig. 4). It should be noted that the onset of magnetism for sites 1, at $T_{N2} \sim 74 K$, coincides with the appearance of the weak ferromagnetic phase, suggesting that the canting of spins, caused in the triads by the order of sites 1, is related to this ferromagnetism. The $Fe^{2+}(4)$ reveal a hyperfine magnetic field between 74 and 112 K, however, only a weak one, which may be associated with a transferred field from the already magnetically ordered three-leg ladder.

Below 74 K the onset of magnetic order of $Fe^{2+}(1)$ triggers the canting of the spins of the Fe ions, inside the triads, and thus indirectly of the $Fe^{2+}(4)$. In addition (see Fig. 4), there is a clear increase of the B_{hf} values, for the species $Fe^{3+}(3)^*$, as compared with those values for the other irons of the triad.

There are only minor changes in the magnetic patterns below 50 K where, according to magnetization and also to neutron data, an antiferromagnetic state is formed. Notably, between 74 and 50 K, there occurs a severe change in isomer shifts and quadrupole interactions of the ions forming the triad [see Figs. 3(a) and 3(b)]. Below 50 K the mixed valent sites at higher temperatures can be clearly assigned to divalent and trivalent iron, with the parameters of $Fe^{3+}(3)^{**}$ now being identical to $Fe^{3+}(3)^*$. This indicates that, in this temperature range, the electronic exchange has become negligible and the extra electron in the triad is localized at site 2, meaning that charge order is established in the triads.

When extrapolating the magnetic hyperfine fields from this low temperature regime to higher temperatures, one would expect the magnetic hyperfine field to vanish at a higher temperature than the actually measured Néel temperature T_{N1} . Therefore, one may also suspect that some short-range order is left above the experimentally determined T_{N1} . There are also indications for this from magnetization data.⁴

As main results drawn from our Mössbauer study in the absence of an applied field, we can summarize: Below 112 K all the Fe ions, except the Fe^{2+} ions in sites 1, order magnetically. There is only a weak coupling of three-leg ladders of triads consisting of trivalent iron and mixed valent pairs of iron and divalent iron, attached to the triads in sites 4. The mixed valent character of the pairs implies some ferromagnetic coupling of them. This means that the overall antiferromagnetism may be established by an alternating spin arrangement of neighboring triads.

At 74 K an unusual increase of B_{hf} and a change in its direction with respect to the main axis of the electric field

gradient is observed for all the ordered Fe ions. In addition, the Fe^{2+} in sites 1 order magnetically below this temperature. We suggest that the appearance of weak ferromagnetism below $T_{N2}=74$ K is related to these findings.^{6,7}

Below 50 K all the Fe ions spins are locked and the system returns to an antiferromagnetic state, as inferred from bulk magnetization.⁶ This coincides with charge ordering, which results in localized iron states over the three-dimensional structure of the Fe ludwigite.³

In the reentrant antiferromagnetic state below 50 K, the spin of $\text{Fe}^{2+}(1)$ do not contribute to the total magnetization. We therefore propose that spins in the chains of $\text{Fe}^{2+}(1)$ ions possess some degree of frustration, resulting in a spin-glass-like magnetic configuration. Spin-glass formation also was observed in the Fe–Cu and Fe–Ni ludwigites, where it is due to positional disorder.^{14,15}

Next we want to describe the electronic structure in the different temperature regimes and we will return to the magnetic structure latter.

C. Electronic structure in different temperature regimes

The thermal variations of the δ_{IS} and ΔE_Q values are shown in Figs. 3(a) and 3(b), respectively. The δ_{IS} values are corrected for second-order Doppler shift.¹¹ At each temperature, the isomer shift values of the iron sites with the same oxidation state are identical. The isomer shifts of Fe^{2+} in positions 1 and 4 remains almost constant with increasing temperature [see Fig. 3(a)], indicating that the divalent ions, which are outside of the triads, are not participating in charge ordering. This is an agreement with the fact that the distances between $\text{Fe}^{2+}(1)$ and $\text{Fe}^{2+}(4)$ and the trivalent iron neighbors in the triads are >3 Å,¹⁶ which impedes electron exchange. Considering the triads as formed by three Fe^{3+} sharing an extra electron, one may expect a changing charge behavior along the temperatures as follows. If the electron is at the Fe that is at the middle, this would be a Fe^{2+} , and the remaining two Fe can have a similar electronic structure close to Fe^{3+} . If the electron is shared or tunneling between two Fe (the middle one with the left or right one), they can have similar charge. This is the case for $\text{Fe}^{2+}(2)$ and $\text{Fe}^{3+}(3)^{**}$. The remaining Fe of the triad, which does not participate in this process, would have more trivalent character (meaning a smaller isomer shift value), as is found for $\text{Fe}^{3+}(3)^*$.

We now discuss our data starting from 4 K and going to the higher temperatures. From Fig. 3 we clearly see the difference in the electronic structure of the three iron sites belonging to the triad. Three ranges of temperatures are to be considered. Below 50 K the triad sites, attributed to $\text{Fe}^{3+}(3)^*$ and $\text{Fe}^{3+}(3)^{**}$, have the same δ_{IS} . The value is typical for Fe^{3+} in the high-spin state ($S=5/2$), while the $\text{Fe}^{2+}(2)$ is close to high-spin Fe^{2+} . This indicates that, at these low temperatures, there is negligible charge transfer from $\text{Fe}^{2+}(2)$. Notice that the magnetic arrangement in the triads, as obtained by neutron scattering⁹ at 5 K, is such that the two magnetic moments at sites $\text{Fe}^{3+}(3)^*$ and $\text{Fe}^{3+}(3)^{**}$ are parallel and both in turn are antiparallel to that at site $\text{Fe}^{2+}(2)$. This antiferromagnetic coupling inside the triad is not favorable for the electron exchange between the three sites. Above

50 K, the δ_{IS} of $\text{Fe}^{3+}(3)^*$ and $\text{Fe}^{3+}(3)^{**}$ are clearly different, with the δ_{IS} of $\text{Fe}^{3+}(3)^{**}$ rising to higher values, typical for iron with an intermediate valence of about 2.5, and the δ_{IS} of $\text{Fe}^{3+}(3)^*$, decreasing to smaller values typical for Fe^{3+} . Furthermore, the δ_{IS} of $\text{Fe}^{2+}(2)$ decreases to values belonging to $\text{Fe}^{2.5+}$. This behavior, for the δ_{IS} , is followed consistently by the corresponding quadrupole interactions. All of these changes start above 50 K and stabilize around 74 K. This temperature range coincides with the appearance of weak ferromagnetism in $\text{Fe}_3\text{O}_2\text{BO}_3$ (see above). It can serve to define a first transition at $T_{N3}=50$ K, where one extra electron can tunnel between two irons on sites 2 and 3 inside the triad, perpendicular to the c direction. To a less extent, this may occur within the triads along the c axis. The charge transfer picture in the triad, among sites $\text{Fe}^{2+}(2)$ and $\text{Fe}^{3+}(3)^{**}$, is compatible with the magnetic measurements, if the magnetic moments at sites $\text{Fe}^{2+}(2)$ and $\text{Fe}^{3+}(3)^{**}$ possess some ferromagnetic component above T_{N3} , as expected from a double-exchange model for ferromagnetism.

Between 74 and about 120 K the quadrupole interactions for $\text{Fe}^{3+}(3)^{**}$ and $\text{Fe}^{2+}(2)$ and the isomer shifts are very similar. This means that the sites 2 and 3, sharing one electron, can hardly be distinguished, probably due to an onset of pair localized hopping. In consequence, the two magnetically inequivalent sites 4 merge to one. This is the range where antiferromagnetism of the triads is found and where the sites 1 outside the triads have lost their magnetic order.

On further increasing the temperature, the isomer shift of the species $\text{Fe}^{2+}(2)$ shows a clear increment at $T=150$ K, reaching again values typical for iron, whereas the δ_{IS} of the species $\text{Fe}^{3+}(3)^*$ and $\text{Fe}^{3+}(3)^{**}$ do not show any pronounced change. We suppose that around this temperature, electron hopping along the c axis is activated adding up to the tunneling and hopping that take place in the ab plane within the triad already at lower temperatures.³ The electron exchange along the c axis is permitted since the distances between positions 2-2 and 3-3, parallel to the c axis, are close to 3.0 Å, which is at the limit where direct exchange can take place.^{3,16} In parallel, there occurs a dramatic change in the transport properties revealing a drop of the activation energy.⁴ The higher activation energy found for low temperatures should however not be related with the electron tunneling in the individual triads, but it is rather connected with the disorder, which at low temperatures, is still frozen and becomes more dynamic above 150 K. At around $T_{CO} \approx 300$ K, a new charge configuration is reached where we can no longer distinguish $\text{Fe}^{3+}(3)^*$ and $\text{Fe}^{3+}(3)^{**}$ from the Mössbauer parameters. Assuming fast charge dynamics, this would imply complete delocalization along the c direction. The fast electronic dynamics leads to an averaged hyperfine interaction at sites 3, which therefore appear indistinguishable. Since sites 2 are still distinctly different, the charge hopping between sites 3 and 2 should stay much slower. In contrast to model calculations given in Ref. 4, the divalent ion of the triad prefers site 2 at all temperatures. In fact, recent x-ray diffraction data have verified the conclusions from the Mössbauer isomer shift and quadrupole data. This preference may be sought in the symmetric position of site 2, which is stabilized for electrostatic reasons probably due to

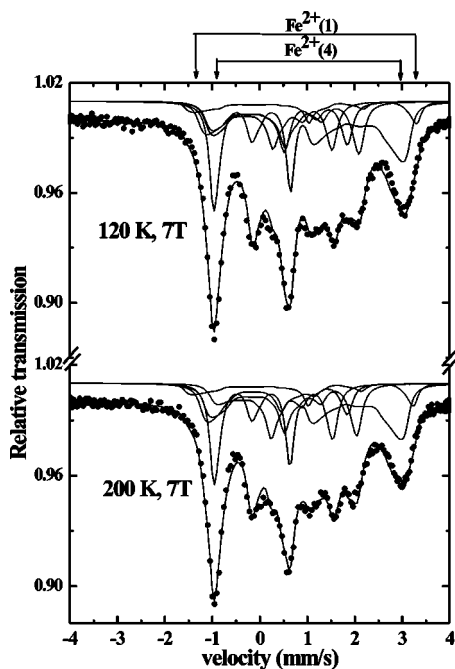


FIG. 6. Mössbauer spectra in the paramagnetic regime under applied external field of 7 T.

the symmetric arrangements of the divalent sites 4 outside the triad.

D. The magnetic spectra under application of an external magnetic field

The analysis of the MS taken under external applied field can give more information about the arrangement of the Fe magnetic moments in different iron sites and their correlation with the electronic states discussed above. We will consider different temperature ranges keeping the same applied field of $B_{ext}=7$ T.

1. (1) $T > T_{N1}$

The only spectra that could be reliably analyzed with a least-squares fitting are the spectra obtained above T_{N1} at 120 and 200 K. It turned out that the hyperfine magnetic fields are fully aligned along the direction of the applied field (see Fig. 6). From the values of the measured hyperfine fields, we conclude that the internal fields of the triad sites 2 and 3 and also of site 4 are opposite to the external field, as expected for a negative internal field of high-spin trivalent iron that is dominated by the contribution from the polarized electron cores. The direction of the field at site 1, however, is parallel to the external field, suggesting a positive hyperfine field probably due to a strong orbital contribution of the divalent iron. The spin contributions appear to be dominant for the other sites, posing some doubts as to the assumption of unquenched orbital momenta for all divalent ions, as proposed in Ref. 4. The values of the internal fields derived for three triad sites and site 4 are roughly as expected from the low temperature saturation fields and a Curie-Weiss temperature T of about -400 to -600 K. This agrees well with the mea-

sured macroscopic magnetization in this temperature range. The magnetic moments governing the local magnetization can be derived from the measured internal fields B_{eff} . Modifying the relation given by Craig *et al.*¹⁷ for free spins by introducing an effective interaction via the Curie-Weiss temperature, we get $B_{eff}=B_{hf}+B_{ext}=B_{sat}g(S+1)\mu_B B_{ext}/[3k_B(T-\Theta)]+B_{ext}$. With this, we find for the triad sites a range of moments $gS\mu_B=12-15\mu_B$, giving further evidence for magnetic short-range order in the triad sites extending far above T_{N1} . From the value of the moment, it is tempting to associate it with ferromagnetic coupling within the three triad sites of individual rungs of the three-leg ladders. This ferromagnetic trimer would also be in agreement with the electron hopping within the triad taking place in this temperature range, as concluded from the isomer shift and quadrupole data. There is definitely no evidence for the formation of nonmagnetic singlets between the trivalent species of the triad, as claimed in Ref. 4. The macroscopically reduced moment found in Ref. 4 may be caused by an antiferromagnetic interaction between the ferromagnetic clusters. This is also reflected in the antiferromagnetic Curie-Weiss temperature found both in the macroscopic magnetization and the Mössbauer measurements. The presence of this short-range order above T_{N1} is probably also the reason that there is detected only a minor change in susceptibility at T_{N1} . From Mössbauer spectroscopy, this transition is picked up due to its sensitivity to the freezing of the fast fluctuating clusters at higher temperatures to the frozen antiferromagnetic state below T_{N1} . These fast fluctuations of cluster magnetizations can be related to the low-dimensional ladder arrangement. From bulk magnetization, there is expected hardly any change in response.

2. (2) $T < T_{N1}$

The MS obtained under applied field below T_{N1} cannot be analyzed fully since the number of correlated fit parameters becomes too big. We restrict ourselves to a qualitative argumentation that may be drawn directly from visual inspection of the MS and from comparison with simulation calculations. Between T_{N1} and T_{N2} [see Fig. 7(a)], we can mainly recognize a broadening of the subspectra referring to the triad sites. The average magnetic hyperfine fields stay unchanged. The relative line intensities within the subspectra are consistent with unpolarized moments, as expected for an antiferromagnetically ordered system in an applied field that is not too large. The hyperfine fields for sites 1 and 4, however, are fully polarized along the applied field with values close to that of the applied field, indicating their still dominantly paramagnetic character.

In the weak ferromagnetic regime below T_{N2} the situation is different: the moments of the triad sites are mainly aligned perpendicular to the external field. This is consistent with an antiferromagnetic arrangement of the triads with a small ferromagnetic component perpendicular to their moments due to canting. Site 4 remains polarized along the external field, again a sign of its weak coupling to the triad. Site 1 seems to have random orientation of moments and supports the picture that site 1 is responsible for the coupling between the walls with domains of varying orientation. Thus, the orien-

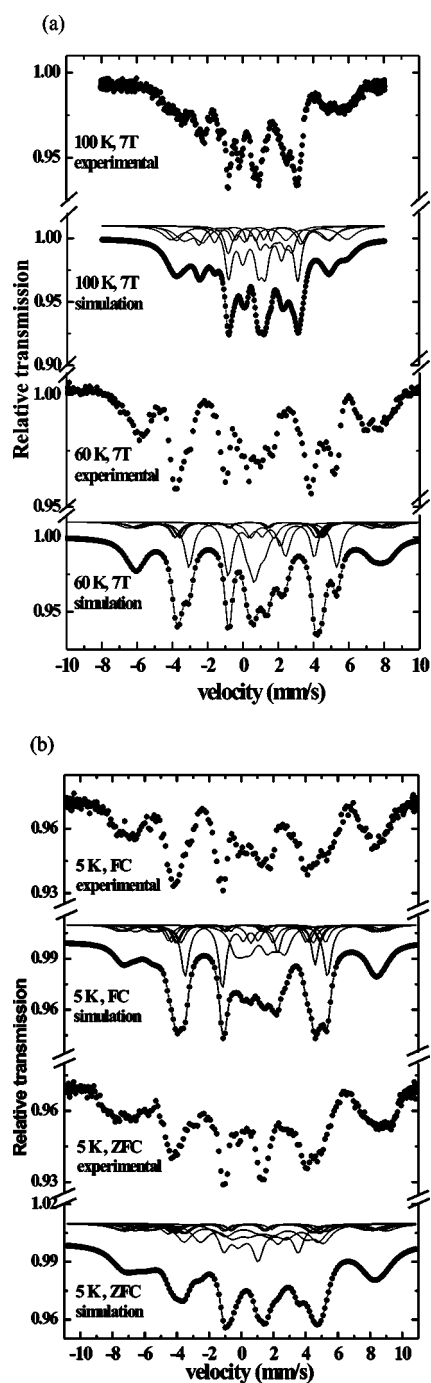


FIG. 7. (a) Mössbauer spectra below T_{N1} in phases AF1 and WF under applied magnetic field of 7 T. (b) Mössbauer spectrum at 5 K (AF2) under applied field after zero field cooling (ZFC) and field cooling (FC).

tation of the moments of site 1 is widely distributed.

Below T_{N3} we find again broadened spectra with average values not much changed even under applied field and random moment directions similar to the situation found also above T_{N2} . This is consistent with an overall antiferromagnetic structure. In contrast to a pure antiferromagnet we find, however, a clear change of the MS when comparing spectra obtained after cooling in an applied field and spectra for

which the field was only applied after cooling down to the respective temperature of measurement [see Fig. 7(b)]. The moments of the triad sites are mainly oriented perpendicular to the applied field similar to the situation in the weak ferromagnetic regime. The moments of sites 1 and 4 remain overall randomly directed. This rather speaks for a spin-glassy component.

IV. CONCLUSIONS

The Mössbauer study of the ludwigite $\text{Fe}_3\text{O}_2\text{BO}_3$ has given a series of interesting aspects of the magnetic behavior of this compound which in part need to be related also to its peculiar electronic structure. The three-dimensional antiferromagnetic phase AF2 below 50 K reveals charge order of divalent and trivalent iron within the so-called triads with magnetically inequivalent trivalent sites. The various sites with different canting angles θ of magnetic hyperfine field with respect to the electric field gradient may be caused by a complex directionally modulated structure. FC effects show the presence of some disorder. The weak ferromagnetic phase between 50 and 74 K is characterized by a rearrangement of spin directions as detected from the changes of angles θ . This phase is characterized by a gradual formation of mixed valent pairs in the triads, also implying some ferromagnetic coupling in these pairs. From 74 to 112 K an antiferromagnetic regime (AF1) is entered. Here the sites 1, which are interlinking the ladders formed by the triads, become nonmagnetic, indicating frustration effects and weak coupling to the triads. Sites 4 only reveal weak magnetic hyperfine fields probably of transferred origin. Above 112 K there is strong evidence for short-range magnetic order within small ferromagnetically coupled clusters of the triads (which may be the individual rungs of the ladders). These clusters are antiferromagnetically interacting among themselves. We have shown that charge ordering occurs in Fe ludwigite below $T_{N3}=50$ K. Above 50 K there is some electron tunneling between pairs of sites 2 and 3 in the ab plane of the triad 3-2-3. Above 74 K thermally activated electron hopping becomes more important giving a more homogeneous charge sharing between sites 2 and 3 in the temperature range from 74 to 150 K. Above 150 K there is an onset of hopping between the triads along the c direction with a transition to fast delocalization above $T_{CO}=300$ K. Sites 1 and 4 outside the triads appear not to be affected by this transition. There have been found clear relations with the changes observed in the charge system and the magnetic behavior of the system, e.g., the appearance of the weak ferromagnetic phase and the vanishing of order in the sites 1 and 4 in the antiferromagnetic regime above 74 K.

ACKNOWLEDGMENTS

E. Baggio-Saitovitch and F. J. Litterst are grateful to DAAD/CAPES and DAAD/CNPq for traveling support. E. Baggio-Saitovitch and M. Continentino acknowledge partial support by FAPERJ (Cientistas do Nosso Estado) and MCT (PRONEX 66201998-9).

- *Visitor from the Technische Universität Braunschweig, Germany.
- ¹J. Ruvalds, *Supercond. Sci. Technol.* **9**, 905 (1996).
- ²J. C. Fernandes, R. B. Guimarães, M. A. Continentino, H. A. Borges, J. V. Valarelli, and A. Lacerda, *Phys. Rev. B* **50**, 16 754 (1994).
- ³J. Larrea J., D. R. Sánchez, E. M. Baggio-Saitovitch, and F. J. Litterst, *J. Phys.: Condens. Matter* **13**, L949 (2001).
- ⁴M. Mir, J. C. Fernandes, R. B. Guimarães, M. A. Continentino, A. C. Doriguetto, Y. P. Mascarenhas, J. Ellena, E. E. Castellano, R. S. Freitas, and L. Ghivelder, *Phys. Rev. Lett.* **87**, 147201 (2001).
- ⁵J. S. Swinnea and H. Steinfink, *Am. Mineral.* **68**, 827 (1983).
- ⁶R. B. Guimarães, M. Mir, J. C. Fernandes, M. A. Continentino, H. A. Borges, G. Cernicchiaro, M. B. Fontes, D. R. S. Candela, and E. Baggio-Saitovitch, *Phys. Rev. B* **60**, 6617 (1999).
- ⁷J. Larrea J., D. R. Sánchez, E. Baggio-Saitovitch, J. C. Fernandes, R. B. Guimarães, M. A. Continentino, and F. J. Litterst, *J. Magn. Mater.* **226**, 1079 (2001).
- ⁸See T. Moriya, in *Magnetism*, edited by G. T. Rado and H. Suhl (Academic, New York, 1963), Vol. 1, p. 85.
- ⁹J. P. Attfield, J. F. Clarke, and D. A. Perkins, *Physica B* **180**, 581 (1992).
- ¹⁰A. P. Douvalis, A. Moukarika, T. Bakas, G. Kallias, and V. Paefthymiou, *J. Phys.: Condens. Matter* **14**, 3302 (2002).
- ¹¹N. N. Greenwood and T. C. Gibb, *Mössbauer Spectroscopy* (Chapman and Hall, London, 1971).
- ¹²J. C. Fernandes, R. B. Guimarães, M. A. Continentino, L. Ghivelder, and R. S. Freitas, *Phys. Rev. B* **61**, R850 (2000).
- ¹³J. Van Dongen Torman, R. Jannathan, and J. M. Trooster, *Hyperfine Interact.* **1**, 135 (1975).
- ¹⁴M. A. Continentino, J. C. Fernandes, R. B. Guimarães, H. A. Borges, A. Suplice, J. L. Tholence, J. L. Siquiera, J. B. M. da Cunha, and C. A. dos Santos, *Eur. Phys. J. B* **9**, 613 (1999).
- ¹⁵J. C. Fernandes, R. B. Guimarães, M. A. Continentino, H. A. Borges, A. Suplice, J. L. Tholence, J. L. Siquiera, I. Zawislak, J. B. M. da Cunha, and C. A. dos Santos, *Phys. Rev. B* **58**, 287 (1998).
- ¹⁶J. Goodenough, *Magnetism and the Chemical Bond* (Wiley Interscience, New York, 1965).
- ¹⁷P. P. Craig, D. E. Nagle, W. A. Steyert, and R. D. Taylor, *Phys. Rev. Lett.* **9**, 12 (1962).